

Exclusive diffractive electroproduction of dijets in collinear factorization

V. M. Braun

Institut für Theoretische Physik, Universität Regensburg, D-93040 Regensburg, Germany

D. Yu. Ivanov

Sobolev Institute of Mathematics, 630090 Novosibirsk, Russia

(Dated: November 6, 2018)

Exclusive electroproduction of hard dijets can be described within the collinear factorization. This process has clear experimental signature and provides one with an interesting alternative venue to test QCD description of hard diffractive processes and extract information on generalized nucleon parton distributions. In this work we present detailed leading-order QCD calculations of the relevant cross sections, including longitudinal momentum fraction distribution of the dijets and their azimuthal angle dependence.

PACS numbers: 12.39.Hg, 12.39.St

I. INTRODUCTION

The QCD description of hard diffraction presents an interesting challenge at the crossroads of soft and hard physics and appeals for a synthesis of various theoretical approaches. In particular diffractive exclusive dijet production in deep-inelastic lepton-nucleon scattering has attracted considerable attention [2, 3, 4, 5]. This process can intuitively be visualized as the incident virtual photon disintegration into a quark-antiquark pair with large and opposite transverse momenta

$$e(l)p(p) \rightarrow e(l')q(q_1)\bar{q}(q_2)p(p'). \quad (1)$$

Here l, l' and p, p' are the initial and the final momenta of the lepton and the nucleon, respectively, while q_1 and q_2 are the jet momenta which to the tree level accuracy can be identified with the momenta of the outgoing quark and antiquark, see Fig. 1. In the following discussion we will use conventional variables

$$q = l - l', \quad q^2 = -Q^2, \quad x_{Bj} = \frac{Q^2}{2(p \cdot q)}, \quad y = \frac{(q \cdot p)}{(l \cdot p)} \quad (2)$$

and neglect the proton mass whenever it is possible.

Our interest to the reaction in (1) is twofold. First, this process provides one with a sensitive probe of the generalized gluon parton distribution (GPD) in the nucleon [6, 7], see e.g. [8]. In this quality, the dijet production with large invariant mass is complementary to e.g. exclusive ρ -meson production and may offer some advantages because it is likely to be less affected by higher twist effects. Second, a quantitative understanding of dijet electroproduction is imperative in order to address more ambitious and theoretically more

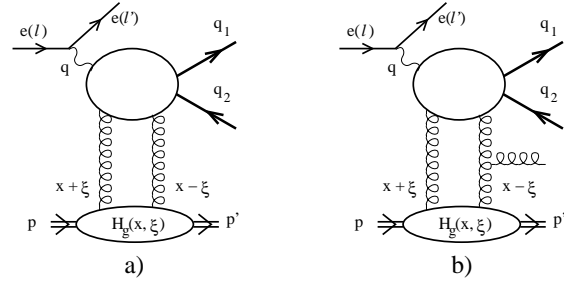


FIG. 1: Kinematics of hard diffractive dijet production

challenging cases of hard dijet production by incident pions [9, 10, 11, 12, 13, 14] and real photons [13, 15]. Another very important extension is exclusive dijet production in pp collisions, where one can study many aspects relevant for exclusive diffractive Higgs production [16]. In the future, there might also be an interesting opportunity to study spin asymmetries in dijet production at eRHIC accelerator, see e.g. [17].

In theory, *exclusive* production is defined as the process in which the invariant energy M^2 deposited in the two narrow angular regions (jet cones), $M^2 = (q_1 + q_2)^2$, almost coincides with the total invariant mass $M_{\text{diff}}^2 = (p + q - p')^2$ of the diffractively produced system, $M^2 \geq (1 - \epsilon)M_{\text{diff}}^2$, with $\epsilon \ll 1$ serving as an infrared cutoff. In existing experiments, diffractive events are usually defined by the presence of large rapidity gaps in the hadronic final state, and main observation that triggered the interest to hard diffraction has been that the probability of large rapidity gaps is not exponentially suppressed. Somewhat imprecisely, we will refer to dijet production under the condition of a large rapidity gap in the hadronic final state as *inclusive* production. There are arguments that inclusive diffraction production of dijets with large

invariant mass is dominated by processes like the one shown in Fig. 1b with a gluon (gluons) emitted from the gluon ladder (pomeron) in the t -channel. The gluon in Fig. 1b is emitted preferably in the central rapidity region, which corresponds to the case $M_{\text{diff}}^2 \gg M^2$.

The experimental distinction between exclusive and inclusive dijets proves to be an intricate problem. One possibility to make such a separation would be to study the corresponding event shapes, for example, by imposing a suitable cutoff in the heavy jet mass. Another proposal [12] is to identify the exclusive dijet final state by requiring that the jet transverse momenta are compensated to a high accuracy within the diffractive cone and making some additional cuts. This approach seems to work for the case of coherent dijet production from nuclei by incident pions, and for photoproduction the corresponding experimental program is proposed for HERA [13].

The dijet electroproduction at high Q^2 offers itself as the simplest process of this kind, in which QCD collinear factorization can be established and allows one to make well defined and stable predictions for the exclusive dijet longitudinal momentum fraction distributions as well as the dependence on the azimuthal angle between the jet and the lepton planes; these distributions can be used to test the separation of exclusive dijets from the inclusive sample. The purpose of this paper is to work out the necessary cross sections and present detailed calculations for HERA kinematics. A similar program was suggested in Ref. [4] where a different theoretical approach based on k_t -factorization was used. Our calculation is also similar to [5] where hard exclusive meson pair production has been considered. A comparison of this earlier works with our results is done below in the text.

Throughout this paper we will work in a reference frame where the virtual photon and the proton collide back-to-back. We will neglect proton mass whenever possible, $p^2 = p'^2 \rightarrow 0$, and choose the (almost) light-like incident proton momentum p_μ to be in “plus” direction. It is convenient to introduce another light-like vector in “minus” direction:

$$q'_\mu = q_\mu + x_{Bj} p_\mu, \quad q'^2 = 0, \quad (q' \cdot p) = (q \cdot p), \quad (3)$$

so that e.g. the lepton momenta can be decomposed in the two light-cone components $\sim p, q'$ and the orthogonal plane:

$$l_\mu = \frac{1}{y} q'_\mu + \frac{(1-y)x_{Bj}}{y} p_\mu + l_{\perp\mu},$$

$$l'_\mu = \frac{1-y}{y} q'_\mu + \frac{x_{Bj}}{y} p_\mu + l_{\perp\mu},$$

$$l_\perp^2 = \frac{1-y}{y^2} Q^2. \quad (4)$$

Note that l_\perp^2 is defined as the square of the transverse plane vector, i.e. with opposite sign compared to the square of the corresponding four-vector.

Further, let W be the invariant c.m. energy of the virtual photon-proton scattering subprocess

$$\gamma^*(q) p(p) \rightarrow q(q_1) \bar{q}(q_2) p(p'), \quad (5)$$

i.e. $s_{\gamma^*p} = (q+p)^2 = W^2$. We define

$$\Delta = p' - p, \quad P = \frac{p+p'}{2}, \quad t = \Delta^2,$$

$$(q-\Delta)^2 = M^2, \quad x_{Bj} = \frac{Q^2}{W^2 + Q^2}. \quad (6)$$

To our approximation $M^2 = (q_1 + q_2)^2$ is an invariant mass of the diffractively produced system.

II. KINEMATICS OF EXCLUSIVE DIJET PRODUCTION

We introduce two light-like vectors

$$n_+^2 = n_-^2 = 0, \quad n_+ n_- = 1 \quad (7)$$

in such a way that

$$p = (1 + \xi) W n_+ \equiv p_+,$$

$$q' = \frac{Q^2 + W^2}{2W(1 + \xi)} n_- \equiv q'_-, \quad (8)$$

where ξ is the usual asymmetry parameter [6] which defines, in the scaling limit, the plus component of the momentum transfer

$$\xi = \frac{p_+ - p'_+}{p_+ + p'_+}. \quad (9)$$

Any four-vector a^μ is decomposed as

$$a^\mu = a^+ n_+^\mu + a^- n_-^\mu + a_\perp^\mu, \quad a^2 = 2 a^+ a^- - a_\perp^2. \quad (10)$$

Then, in particular

$$q = \frac{Q^2 + W^2}{2W(1 + \xi)} n_- - W(1 + \xi) x_{Bj} n_+,$$

$$p' = (1 - \xi) W n_+ + \frac{\Delta_\perp^2}{2(1 - \xi) W} n_- + \Delta_\perp. \quad (11)$$

We consider the case when jet transverse momenta are compensated, $(q_1 + q_2)_\perp = -\Delta_\perp = 0$ so that

the last two terms in the second equation in (11) can be dropped. The momenta of the dijets can be written as

$$\begin{aligned}
q_1 &= z \frac{Q^2 + W^2}{2W(1 + \xi)} n_- \\
&\quad + \frac{q_\perp^2 + m^2}{zQ^2} W(1 + \xi) x_{Bj} n_+ + q_\perp, \\
q_2 &= \bar{z} \frac{Q^2 + W^2}{2W(1 + \xi)} n_- \\
&\quad + \frac{q_\perp^2 + m^2}{\bar{z}Q^2} W(1 + \xi) x_{Bj} n_+ - q_\perp, \quad (12)
\end{aligned}$$

where m is the quark mass and z is the relative longitudinal “minus” momentum fraction carried by the quark jet. Here and below we use a shorthand notation

$$\bar{z} = 1 - z.$$

The dijet invariant mass equals

$$(q_1 + q_2)^2 = M^2 = \frac{q_\perp^2 + m^2}{z\bar{z}} \quad (13)$$

and the asymmetry parameter

$$\frac{2\xi}{1 + \xi} = \frac{Q^2 + M^2}{Q^2 + W^2}. \quad (14)$$

For future convenience we introduce the notation

$$\mu^2 = m^2 + z\bar{z}Q^2, \quad (15)$$

and the parameter

$$\beta = \frac{\mu^2}{q_\perp^2 + \mu^2} = \frac{Q^2 + \frac{m^2}{z\bar{z}}}{M^2 + Q^2}, \quad (16)$$

which for light quark jets $m \rightarrow 0$ coincides with the conventional β -parameter used in the description of diffractive deep inelastic scattering, see e.g. [1].

We will calculate the distributions in the angle between the electron scattering and the jets planes, cf. [4, 18]. In order to define this angle we introduce two transverse unit vectors

$$\begin{aligned}
e_x &= (0, 1, 0, 0), \\
e_y &= (0, 0, 1, 0), \quad (17)
\end{aligned}$$

in such a way that the incident lepton transverse momentum (4) is in x -direction, $l_\perp = |l_\perp|e_x$, and the quark jet transverse momentum equals to $q_\perp = |q_\perp|(e_x \cos \phi + e_y \sin \phi)$, see Fig. 2.

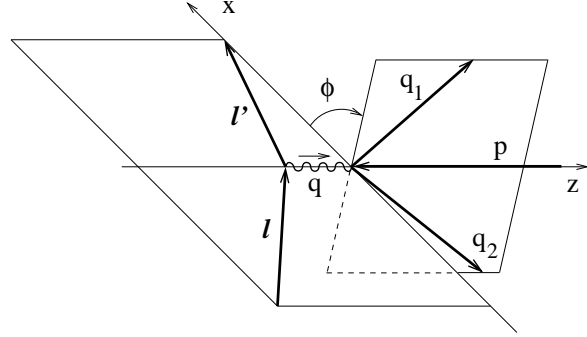


FIG. 2: The azimuthal angle ϕ is defined as the angle between the two planes: one formed by the lepton momenta l, l' and the other one by the jet momenta q_1, q_2 .

The deep inelastic differential cross section is written as

$$\begin{aligned}
d\sigma &= (2\pi)^4 \delta^4(l + p - l' - q_1 - q_2 - p') \\
&\quad \times \frac{|M|^2}{4(l \cdot p)} \frac{d^3 l' d^3 q_1 d^3 q_2 d^3 p'}{(2\pi)^{12} 2l'_0 2q_{1,0} 2q_{2,0} 2p'_0}. \quad (18)
\end{aligned}$$

The amplitude M can be expressed in terms of the amplitude of the photon-nucleon scattering. In the Feynman gauge we have

$$M = \frac{\sqrt{4\pi\alpha_{em}}}{Q^2} \bar{u}(l') \gamma^\mu u(l) g_{\mu\nu} M_{\gamma^*}^\nu. \quad (19)$$

and using gauge invariance can replace the $g_{\mu\nu}$ tensor by the sum of projections on the different possible polarization vectors of the virtual photon:

$$g^{\mu\nu} \rightarrow e_L^\mu e_L^\nu - \sum_{\lambda=x,y} e_{T,\lambda}^\mu e_{T,\lambda}^\nu \quad (20)$$

In what follows we use the longitudinal polarization vector

$$e_L = \frac{Q^2 + W^2}{2WQ(1 + \xi)} n_- + \frac{W}{Q} (1 + \xi) x_{Bj} n_+, \quad (21)$$

and define the transverse polarization vectors as

$$\begin{aligned}
e_T &= 0 \cdot n_+ + 0 \cdot n_- + e_\perp, \\
e_{T,x} &= e_x, \\
e_{T,y} &= e_y. \quad (22)
\end{aligned}$$

Accordingly, we define the photon subprocess amplitudes for different polarizations as

$$\mathcal{A}_L = M_{\gamma^*}^\mu e_{L,\mu}, \quad \mathcal{A}_T = M_{\gamma^*}^\mu e_{T,\mu} \quad (23)$$

and

$$\mathcal{A}_T^x = M_{\gamma^*}^\mu e_{x,\mu}, \quad \mathcal{A}_T^y = M_{\gamma^*}^\mu e_{y,\mu} \quad (24)$$

It is not difficult to show that

$$\frac{d^3 l'}{2l'_0} = \frac{1}{4} dy dQ^2 d\phi_{l'} \quad (25)$$

and the cross section of interest takes the form

$$(2\pi) \frac{d\sigma}{dy dQ^2 d\phi_{l'}} = \frac{\alpha_{em}}{\pi Q^2 y} \left[\frac{4-4y+y^2}{4} |\mathcal{A}_T^x|^2 + \frac{y^2}{4} |\mathcal{A}_T^y|^2 + (1-y) |\mathcal{A}_L|^2 + (2-y) \sqrt{1-y} \text{Re}(\mathcal{A}_T^x \mathcal{A}_L^*) \right] \\ \times \frac{dz d\phi d q_{\perp}^2}{2^9 \pi^4 z \bar{z} (W^2 + Q^2)(W^2 - M^2)} \frac{d\Delta_{\perp}^2 d\phi_{p'}}{2\pi}. \quad (26)$$

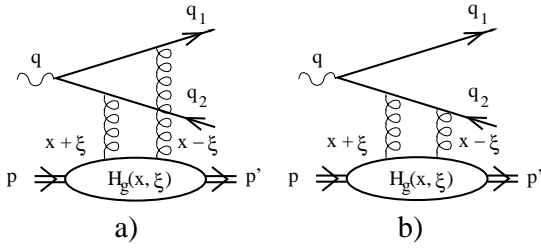


FIG. 3: Gluon contribution to the hard exclusive dijet production

Here $\phi_{p'}$ is the azimuthal angle for the outgoing nucleon. The corresponding integration is trivial so that the factor $d\phi_{p'}/2\pi$ can be replaced by unity for all practical purposes. In the numerical calculation described below we assume the behavior $d\sigma/d\Delta_{\perp}^2 \sim \exp[-b\Delta_{\perp}^2]$ with the universal slope $b = 5 \text{ GeV}^2$.

III. CALCULATION OF THE AMPLITUDES

In this work we calculate the necessary amplitudes to leading order in perturbation theory using collinear factorization. The corresponding diagrams are shown in Fig. 3 and Fig. 4 for the gluon and quark contributions, respectively. In both cases the addition of symmetric diagrams with the permutation of the quark and the antiquark is understood.

In the framework of collinear factorization, the necessary hadronic input is parametrized in terms of generalized parton distributions (GPDs). GPDs are defined as matrix elements of light-ray quark and gluon operators sandwiched between nucleon (proton) states with different momenta [6, 7]:

$$F^q(x, \xi, \Delta^2) =$$

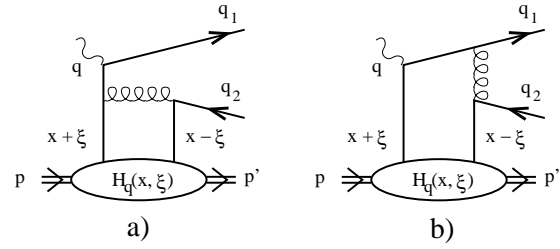


FIG. 4: Quark contribution to the hard exclusive dijet production

$$= \frac{1}{2} \int \frac{d\lambda}{2\pi} e^{ix(Pz)} \langle p' | \bar{q} \left(-\frac{z}{2} \right) \not{n} - q \left(\frac{z}{2} \right) | p \rangle_{z=\lambda n_-} \\ = \frac{1}{2(Pn_-)} \left[\mathcal{H}^q(x, \xi, \Delta^2) \bar{u}(p') \not{n} - u(p) \right. \\ \left. + \mathcal{E}^q(x, \xi, \Delta^2) \bar{u}(p') \frac{i\sigma^{\alpha\beta} n_{-\alpha} \Delta_{\beta}}{2m_N} u(p) \right],$$

$$F^g(x, \xi, \Delta^2) = \\ = \frac{1}{(Pn_-)} \int \frac{d\lambda}{2\pi} e^{ix(Pz)} n_{-\alpha} n_{-\beta} \\ \times \langle p' | G^{\alpha\mu} \left(-\frac{z}{2} \right) G_{\mu}^{\beta} \left(\frac{z}{2} \right) | p \rangle_{z=\lambda n_-} \\ = \frac{1}{2(Pn_-)} \left[\mathcal{H}^g(x, \xi, \Delta^2) \bar{u}(p') \not{n} - u(p) \right. \\ \left. + \mathcal{E}^g(x, \xi, \Delta^2) \bar{u}(p') \frac{i\sigma^{\alpha\beta} n_{-\alpha} \Delta_{\beta}}{2m_N} u(p) \right]. \quad (27)$$

Here $u(p)$ and $\bar{u}(p')$ are the nucleon spinors. In both cases insertion of the path-ordered gauge factor between the field operators is implied. The momentum fraction x , $-1 \leq x \leq 1$, parametrizes parton momenta with respect to the symmetric momentum $P = (p + p')/2$. In the forward limit, $p' = p$, the contributions proportional to the functions $\mathcal{E}^q(x, \xi, \Delta^2)$ and $\mathcal{E}^g(x, \xi, \Delta^2)$ vanish, whereas the distributions $\mathcal{H}^q(x, \xi, \Delta^2)$ and $\mathcal{H}^g(x, \xi, \Delta^2)$ re-

duce to the ordinary quark and gluon densities:

$$\begin{aligned}\mathcal{H}^q(x, 0, 0) &= q(x) \quad \text{for } x > 0, \\ \mathcal{H}^q(x, 0, 0) &= -\bar{q}(-x) \quad \text{for } x < 0; \\ \mathcal{H}^g(x, 0, 0) &= x g(x) \quad \text{for } x > 0.\end{aligned}\quad (28)$$

Note that the gluon GPD is an even function of x , $\mathcal{H}^g(x, \xi, \Delta^2) = \mathcal{H}^g(-x, \xi, \Delta^2)$.

The calculation is relatively straightforward so that we omit the details. The $\gamma^* N$ scattering amplitude for the longitudinal photon polarization can be written as

$$\mathcal{A}_{\gamma_L}^g = -\frac{4\pi\alpha_s\sqrt{4\pi\alpha_{em}}e_q\delta_{ij}}{N_c}\frac{z\bar{z}QW}{[q_\perp^2+\mu^2]^2}\bar{u}(q_1)\not{n}_+v(q_2)(I_L^g+2C_F I_L^q), \quad (29)$$

where

$$\begin{aligned}I_L^g &= \int_{-1}^1 dx F^g(x, \xi, \Delta^2) \left(\frac{2\xi\bar{\beta}}{(x+\xi-i\epsilon)^2} + \frac{2\xi\bar{\beta}}{(x-\xi+i\epsilon)^2} - \frac{2\xi(1-2\beta)}{(x+\xi-i\epsilon)(x-\xi+i\epsilon)} \right), \\ I_L^q &= \int_{-1}^1 dx F^q(x, \xi, \Delta^2) \left(\frac{2\xi\bar{z}}{(x+\xi-i\epsilon)} + \frac{2\xi z}{(x-\xi+i\epsilon)} \right).\end{aligned}\quad (30)$$

We denote $\bar{\beta} = 1 - \beta$, $u(q_1), v(q_2)$ are the quark spinors and δ_{ik} stands for the colors of the outgoing quarks, $C_F = (N_c^2 - 1)/2N_c$ where $N_c = 3$ for QCD. For the transverse photon polarization we obtain

$$\begin{aligned}\mathcal{A}_{\gamma_T} &= -\frac{2\pi\alpha_s\sqrt{4\pi\alpha_{em}}e_q\delta_{ij}}{N_c}\frac{W}{[q_\perp^2+\mu^2]^2}\left\{ -\bar{u}(q_1)[m\not{\epsilon}_\perp]\not{n}_+v(q_2)I_L^g \right. \\ &\quad \left. + \bar{u}(q_1)\not{q}_\perp\not{\epsilon}_\perp\not{n}_+v(q_2)(2C_F I_T^{q_1} + \bar{z}I_T^g) + \bar{u}(q_1)\not{\epsilon}_\perp\not{q}_\perp\not{n}_+v(q_2)(2C_F I_T^{q_2} - zI_T^g) \right\},\end{aligned}\quad (31)$$

with

$$\begin{aligned}I_T^g &= \int_{-1}^1 dx F^g(x, \xi, \Delta^2) \left(\frac{\xi(1-2\beta)}{(x+\xi-i\epsilon)^2} + \frac{\xi(1-2\beta)}{(x-\xi+i\epsilon)^2} + \frac{4\xi\beta}{(x+\xi-i\epsilon)(x-\xi+i\epsilon)} \right), \\ I_T^{q_1} &= \int_{-1}^1 dx F^q(x, \xi, \Delta^2) \left(\frac{2\xi z\bar{z}}{(x-\xi+i\epsilon)} - \frac{2\xi\beta\bar{z}^2}{\bar{\beta}(x+\xi-i\epsilon)} + \frac{2\xi\bar{z}^2}{\bar{\beta}(x-\xi(1-2\beta)-i\epsilon)} \right), \\ I_T^{q_2} &= \int_{-1}^1 dx F^q(x, \xi, \Delta^2) \left(\frac{2\xi\beta z^2}{\beta(x-\xi+i\epsilon)} - \frac{2\xi z\bar{z}}{(x+\xi-i\epsilon)} - \frac{2\xi z^2}{\beta(x+\xi(1-2\beta)+i\epsilon)} \right).\end{aligned}\quad (32)$$

In both cases the expressions are written for one quark flavor. The quark mass corrections have been omitted for quark contributions, cf. Fig. 4, and only have to be taken into account in the charm- or eventually beauty-quark production in the gluon contributions shown in Fig. 3. Note that for heavy quark jets our definition of the β -parameter (16) differs somewhat from the conventional β -parameter used in the description of diffraction scattering.

Using the virtual photon amplitudes given in (29) and (31) we calculate the dijet cross section, summed over helicities and color of the produced $(q\bar{q})$ pair:

$$\frac{d\sigma}{dydQ^2} = \frac{\alpha_{em}}{\pi Q^2 y} \left[\frac{1+(1-y)^2}{2} d\sigma_T - 2(1-y)\cos 2\phi d\sigma_{TT} + (1-y)d\sigma_L - (2-y)\sqrt{1-y}\cos\phi d\sigma_{LT} \right] \quad (33)$$

where

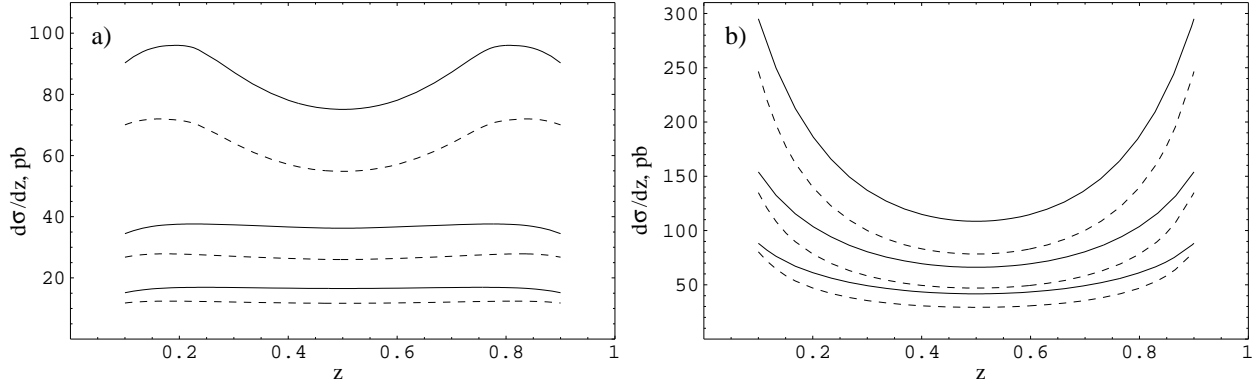


FIG. 5: Longitudinal momentum fraction distribution of the dijets, summed over all quark flavors $q = u, d, s, c$. The three curves correspond to different minimum dijet transverse momenta; from above to below: $q_0 = 1.25, 1.5, 1.75$ GeV. The solid and the dashed curves correspond to a model for the generalized parton distribution based on the leading-order CTEQ6L and MRST2001LO leading-order parton distributions, respectively. The results shown on panel a) correspond to the calculation with a cutoff $Q^2/(Q^2 + M^2) > 0.5$, whereas the ones shown on panel b) are calculated without such a cutoff. In the latter case we take $Q^2 > 10$ GeV².

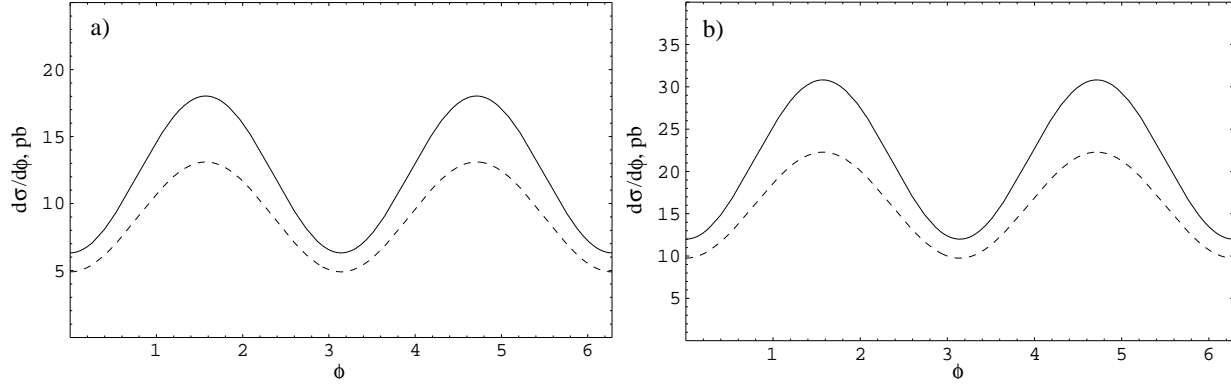


FIG. 6: Azimuthal angle distribution of the dijets, $q_\perp > 1.25$ GeV, summed over all quark flavors $q = u, d, s, c$. Identification of the panels and curves is the same as in Fig. 5, see also text.

$$\begin{aligned}
 d\sigma_T &= \left[\frac{m^2}{q_\perp^2} |I_L^g|^2 + |\bar{z}I_T^g + 2C_F I_T^{q_1}|^2 + |zI_T^g - 2C_F I_T^{q_2}|^2 \right] d\sigma, \\
 d\sigma_{TT} &= \text{Re} \left[(\bar{z}I_T^g + 2C_F I_T^{q_1})(zI_T^g - 2C_F I_T^{q_2})^* \right] d\sigma, \\
 d\sigma_L &= 4(z\bar{z})^2 \frac{Q^2}{q_\perp^2} |I_L^g + 2C_F I_L^q|^2 d\sigma, \\
 d\sigma_{LT} &= 2(z\bar{z}) \frac{Q}{q_\perp} \text{Re} \left[(I_L^g + 2C_F I_L^q)((1-2z)I_T^g + 2C_F(I_T^{q_1} + I_T^{q_2}))^* \right] d\sigma
 \end{aligned} \tag{34}$$

and

$$d\sigma = \frac{\alpha_{em} \alpha_s^2 e_q^2}{16\pi N_c (1 - \xi^2)} \frac{q_\perp^2 dq_\perp^2 d\Delta_\perp^2 dz d\phi}{(q_\perp^2 + \mu^2)^4}. \tag{35}$$

The same cross section in the k_\perp -factorization approach of Ref. [3] can be recovered by neglecting the double-pole terms in I_L^g , I_T^g , in (30), (32),

taking into account the imaginary part only

$$\begin{aligned}
 I_L^g &\rightarrow i\pi \cdot 2(1 - 2\beta) F^g(\xi, \xi, \Delta^2), \\
 I_T^g &\rightarrow -i\pi \cdot 4\beta F^g(\xi, \xi, \Delta^2),
 \end{aligned} \tag{36}$$

and also neglecting the quark mass and quark contributions altogether. The result coincides with the

expression given in [4], except for the sign in the last term in (33) $\sim \cos \phi$. Our sign agrees with an independent calculation in [18] in a kind of a two-gluon exchange model. (To be precise, our definition of ϕ differs in sign from the definition used in [18].)

IV. NUMERICAL RESULTS

The numerical results presented below are calculated using a model for the generalized parton distributions that is based on CTEQ6L [20] (solid curves) and MRST2001LO [21] (dashed curves) leading-order parton distributions at the scale 4 GeV². For our analysis we neglect the contributions of \mathcal{E}^q and \mathcal{E}^g , see (27), since their contributions is expected to be minor in the HERA energy range. The \mathcal{H}^q and \mathcal{H}^g distributions are modeled using the parametrization in terms of the so-called double distributions using an ansatz proposed in [22] with profile functions chosen to be $\pi(x, y) = 6y(1-x-y)(1-x)^{-3}$ for quarks and $\pi(x, y) = 30y^2(1-x-y)^2(1-x)^{-5}$ for gluons. We use the two-loop running QCD coupling corresponding to the value $\alpha_s(M_Z) = 0.1165$. For the scale of the running coupling we take $m^2 + q_\perp^2 + z\bar{z}Q^2$ for the c -quark, and $q_\perp^2 + z\bar{z}Q^2$ for the light quark production. The charm quark mass is taken to be $m_c = 1.25$ GeV. We plot one-dimensional differential cross sections obtained by integrating (33) over the remaining variables. The distributions over the longitudinal momentum fraction of the dijets (“ z -distributions”) are shown for the integral over all azimuthal angles, $0 < \phi < 2\pi$, whereas for the azimuthal angle distributions (“ ϕ -distributions”) we integrate in the range $0.1 < z < 0.9$. We take integration limits in the deep-inelastic y -variable $0.1 < y < 0.4$ which roughly corresponds to the energy interval $W = 100 \div 200$ GeV. We also integrate over the dijet transverse momenta $q_\perp^2 > q_0^2$ with three choices for the cutoff: $q_0 = 1.25, 1.5, 1.75$ GeV, and over Q^2 in the range $Q^2 = 10 \div 500$ GeV². In addition, we introduce a cutoff on the invariant dijet mass $M^2 < Q^2$ alias for the diffractive DIS β -parameter

$$\beta^{\text{DDIS}} = Q^2/(Q^2 + M^2) > 0.5$$

(cf. (16)), which is supposed to facilitate the extraction of the exclusive diffractive dijet cross section experimentally. Indeed, in the region of large β^{DDIS} radiation of an additional gluon (gluons) in the final state, as shown in Fig.1b, represents a radiative correction $\mathcal{O}(\alpha_s)$ to the main process, the $q\bar{q}$ pair production. At the same time, for small

β^{DDIS} radiation of gluons is enhanced by large logarithms of the energy and is numerically very important. It leads to events which have a topology of inclusive diffractive dijet production. In this case a special experimental procedure is needed to isolate the exclusive contribution. Last but not least, it is worthwhile to mention that all calculations in this work refer to the parton-level cross sections, hadronization effects are not taken into account. We also average over the quark and the antiquark jets, since their distinction is very difficult experimentally. With this averaging, the last term $\sim \sigma_{LT}$ in (33) drops out.

The longitudinal momentum fraction and the azimuthal angle distributions of the dijets, summed over all quark flavors $q = u, d, s, c$, are shown in Fig. 5 and Fig. 6, respectively. Note that the z -distributions are affected strongly by the cutoff $\beta^{\text{DDIS}} > 0.5$ [23], while the ϕ -distributions remain qualitatively the same. This effect is easy to understand and is due to a strong kinematic suppression of small $z \rightarrow 0$ and large $z \rightarrow 1$ longitudinal momentum regions that correspond to large masses of the diffractively produced system. The difference between the solid and the dashed curves is mainly in the absolute normalization and it arises because of the different small- x behavior of the CTEQ6L and MRST2001LO gluon distributions.

We expect that the accuracy of our calculation is mainly limited by the size of the next-to-leading order (NLO) corrections. E.g. for vector meson electroproduction the NLO corrections were found to be large [24]. The uncertainties involved in the modeling of generalized (off-forward) parton distributions are probably less important in the HERA energy range that we consider in this work.

The same distributions are plotted in Fig. 7 and Fig. 8 for the contributions of c -quark jets separately. Note that the cutoff $\beta^{\text{DDIS}} > 0.5$ leads to a dramatic reduction of the cross section in this case, so that the c -quark contribution to the distributions in Fig. 5a and Fig. 6a is rather small.

As it can be expected, the dijet production is dominated by the contribution of transverse photon polarization, $d\sigma_T$ in Eq. (33). The contribution of the longitudinal polarization, $d\sigma_L$, is shown separately in Fig. 9 for the case $q_\perp > 1.5$ GeV. It is seen that the relative weight of the longitudinal contribution is effectively enhanced by the cutoff $\beta^{\text{DDIS}} > 0.5$ (since $d\sigma_T$ is peaked at small and large z and is strongly suppressed in the end point regions by the cutoff).

In addition, in Fig. 10 we show the y -distribution of the cross section, integrated over the longitudinal momentum fraction of the jets, and over the

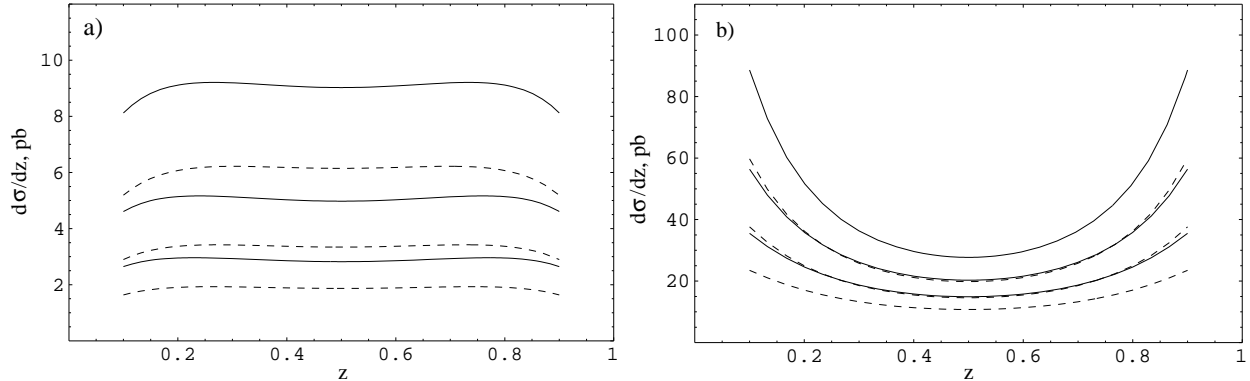


FIG. 7: Same as in Fig. 5, but for charmed quark dijets only.

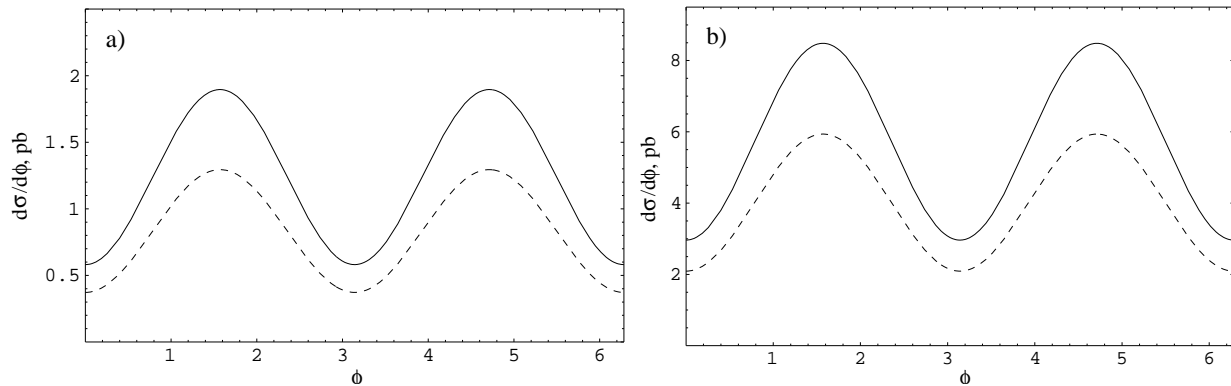


FIG. 8: Same as in Fig. 6, but for charmed quark dijets only.

azimuthal angle. This plot represent, essentially, the energy dependence of the cross section of virtual photon proton scattering (5). In the considered kinematic range we find a steep rise $\sigma_{\gamma^*p} \sim (W^2)^{0.24 \pm 0.26}$ which is typical for hard diffractive processes.

Finally, let us compare our results with the ones obtained earlier in [3, 4] within the k_t -factorization framework. Qualitatively, both collinear factorization and k_t -factorization approaches lead to similar predictions: in particular the same overall Q^2 -scaling, strong energy dependence of the virtual photon proton scattering and the prediction that jets prefer a direction perpendicular to the electron plane. This is not surprising since both techniques coincide in the double logarithmic approximation, see (36). The direct comparison of numerical predictions is difficult due to different cuts used and also different parameterizations for the input gluon parton distributions. It seems, however, that our cross sections tend to be roughly factor of two smaller than the ones reported in [3, 4].

Beyond the double logarithmic approximation there are differences. In collinear factorization quark GPD contributes together with gluon GPD

at the leading order. It turns out that the quark GPD contribution to the amplitude is quite significant. However, we find (as a representative example, see Fig. 11) that it interferes destructively with the gluon GPD contribution and, as the result, the contribution of quark GPD to the cross section cancels to a large extent with the gluon-quark GPDs interference term. Remarkably, this cancellation does not affect much the shape of different distributions, and only results in a moderate increase of the cross section, as compared to the calculation with only the gluon GPD taken into account. One noticeable exception is the longitudinal contribution to the cross section calculated with a β^{DDIS} cutoff. As seen in Fig. 12, neglecting quark GPD contribution underestimates the longitudinal cross section by more than a factor two.

Another difference and a distinct feature of the collinear factorization approach is the appearance of double poles in the coefficient functions for the gluon contributions to both the transverse (32) and the longitudinal (30) amplitudes. Such double-pole terms have no counterparts in the k_t factorization approach. In Fig. 13 we show absolute values of I_T^g and I_L^g as defined in Eqs. (32) and (30), respec-

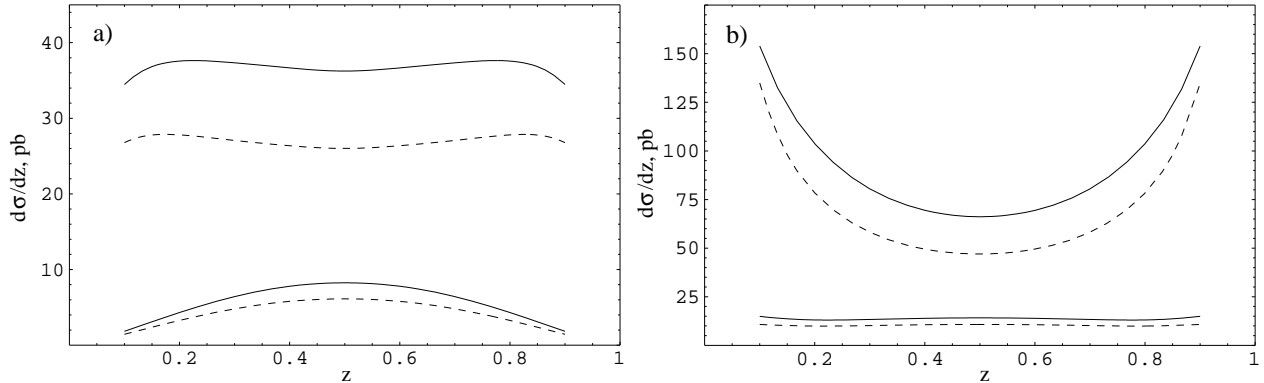


FIG. 9: Longitudinal momentum fraction distribution of the dijets with transverse momentum $q_\perp > 1.5$ GeV, summed over all quark flavors $q = u, d, s, c$ (the two upper curves). The contribution of the longitudinal photon polarization is shown separately (the two lower curves). The calculation is made with (panel a)) and without (panel b)) a cutoff $\beta^{\text{DDIS}} = Q^2/(Q^2 + M^2) > 0.5$. The solid and dashed curves correspond to the CTEQ6L and MRST2001LO parametrizations, respectively.

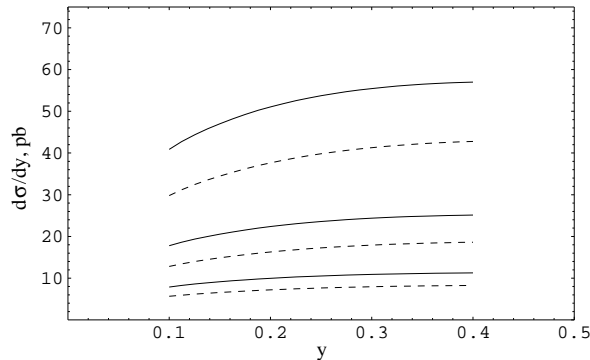


FIG. 10: The y -distribution of the dijets, $y d\sigma/dy$, summed over all quark flavors $q = u, d, s, c$. The calculation is made with a cutoff $Q^2/(Q^2 + M^2) > 0.5$. Identification of the curves is the same as in Fig. 5, see also text.

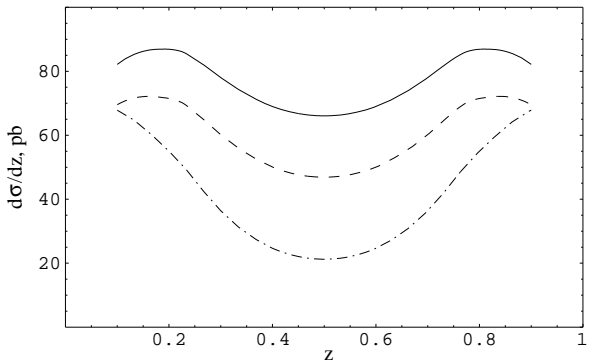


FIG. 11: The longitudinal momentum fraction distribution of the dijets with transverse momentum $q_\perp > 1.25$ GeV summed over light quark flavors $q = u, d, s$. The contributions of the gluon and the quark GPDs are shown by the dashed and the dash-dotted curves, respectively. The sum of all contributions including the quark-gluon interference terms is shown by the solid curve. The calculation is made with a cutoff $\beta^{\text{DDIS}} > 0.5$ and CTEQ6L parton distributions.

tively, calculated for a typical value of the asymmetry parameter $\xi = 0.001$ (9) and for different values of the β -parameter (16). The double pole contributions (shown by dashed curves) are important in the regions where the main single-pole terms vanish: at small β for the transverse amplitude and at $\beta \sim 0.5$ for the longitudinal amplitude.

It is known that at large energies (small x) the amplitudes are predominantly imaginary. Also in our case the imaginary part of the amplitude dominates the dijet cross section. We find however, see Fig. 14, that the contribution of the real part is quite sizable close to the end points, $z \rightarrow 0$ or $z \rightarrow 1$, and especially in the case of the calculation without a β^{DDIS} -cutoff.

V. SUMMARY AND CONCLUSIONS

We have presented a detailed analysis of exclusive diffractive dijet production with large transverse momenta in the framework of QCD collinear factorization. The calculation is done in leading order in the strong coupling. We derived the expressions for the amplitudes for the $q\bar{q}$ pair production by the virtual photon both for the transverse and the longitudinal polarizations and used these results for an extensive numerical study of the differential cross section for HERA kinematics. We have checked that our results for the amplitude are equivalent in the massless quark limit to the

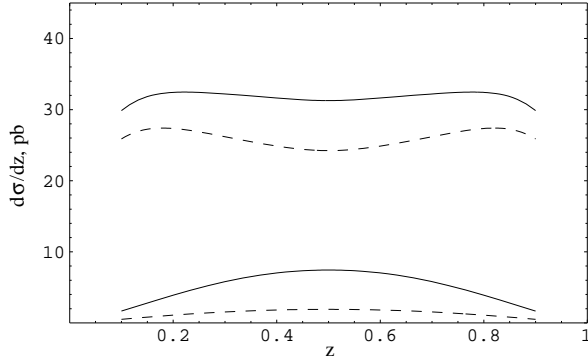


FIG. 12: Longitudinal momentum fraction distribution of the dijets with transverse momentum $q_{\perp} > 1.5$ GeV, summed over all quark flavors $q = u, d, s, c$. The full calculation (solid curves) is compared with the result that includes the contribution of the gluon GPD only (dashed curves). The two lower curves show the longitudinal contribution separately. The calculation is made with a cutoff $\beta^{\text{DDIS}} > 0.5$ and uses CTEQ6L parton distributions.

ones obtained in [5] (where no separation into the transverse and longitudinal contributions is made and different notation used for the GPDs). In the double logarithmic limit our result agrees (except for the sign of $\sim \cos \phi$ term in (33)) with the one obtained in the k_t factorization approach [4].

Experimentally, main challenge in the study of hard dijet production is the necessity to have a clean separation between the exclusive and inclusive channels. Since topology of the event is different in these two cases, such a separation should be possible to achieve using appropriate cuts. The most practical possibility at present is probably to limit the study of diffractive dijet electroproduction to the kinematic region of large β^{DDIS} , say $\beta^{\text{DDIS}} > 0.5$, where the exclusive $q\bar{q}$ production represents the main contribution and radiation of an additional gluon (gluons) in the final state is

suppressed. Our estimates indicate that in the region $\beta^{\text{DDIS}} > 0.5$ the cross section remains sufficiently large and we hope that such an analysis can be done at HERA. As first noted in [4], the azimuthal angle distribution of the dijets can be used to check the separation of the exclusive sample: exclusive jets prefer a direction perpendicular to the electron scattering plane whereas in the inclusive case the distribution is peaked in this plane. We find that the azimuthal angle distribution is stable to various cuts and is not very sensitive to the input GPDs, so it can indeed be used as a useful trigger.

Though quark GPDs contribute significantly to the amplitude, we observe a large cancellation between the square of the quark contribution and the gluon-quark GPDs interference term in the cross section. As the result, both the magnitude of the cross section and the shape of different distributions appear to be not very sensitive to the presence of quark GPD contributions (in the studied energy range). This finding further strengthens the existing expectations (see e.g. [8]) that exclusive diffractive dijet production may offer an interesting possibility to constrain the generalized gluon parton distribution at small x_B .

Acknowledgements

We are grateful to D. Ashery for the questions that initiated this work and valuable correspondence. Our special thanks are due to M. Diehl for reading the manuscript and important remarks. D.I. also thanks the QCD theory group of the University of Regensburg for warm hospitality. Work of D.I. was partially supported by grants RFBR-05-02-16211, NSh-2339.2003.2 and by the DFG grant 436RUS113/754/0-1 “Hard diffractive processes in QCD”.

-
- [1] C. Adloff *et al.* [H1 Collaboration], *Eur. Phys. J. C* **6**, 421 (1999).
 - [2] N. N. Nikolaev and B. G. Zakharov, *Phys. Lett. B* **332**, 177 (1994).
 - [3] J. Bartels, H. Lotter and M. Wusthoff, *Phys. Lett. B* **379**, 239 (1996) [Erratum-ibid. *B* **382**, 449 (1996)].
 - [4] J. Bartels, C. Ewerz, H. Lotter and M. Wusthoff, *Phys. Lett. B* **386**, 389 (1996).
 - [5] B. Lehmann-Dronke, M. Maul, S. Schaefer, E. Stein and A. Schafer, *Phys. Lett. B* **457**, 207 (1999).
 - [6] M. Diehl, *Phys. Rept.* **388**, 41 (2003).
 - [7] A. V. Belitsky and A. V. Radyushkin, arXiv:hep-ph/0504030.
 - [8] K. Golec-Biernat, J. Kwiecinski and A. D. Martin, *Phys. Rev. D* **58**, 094001 (1998).
 - [9] N. N. Nikolaev, W. Schafer and G. Schwieta, *Phys. Rev. D* **63**, 014020 (2001).
 - [10] V. M. Braun, D. Yu. Ivanov, A. Schafer and L. Szymanowski, *Phys. Lett. B* **509**, 43 (2001); *Nucl. Phys. B* **638**, 111 (2002).
 - [11] V. Chernyak, *Phys. Lett. B* **516**, 116 (2001); V. L. Chernyak and A. G. Grozin, *Phys. Lett. B* **517**, 119 (2001).
 - [12] E. M. Aitala *et al.* [E791 Collaboration], *Phys.*

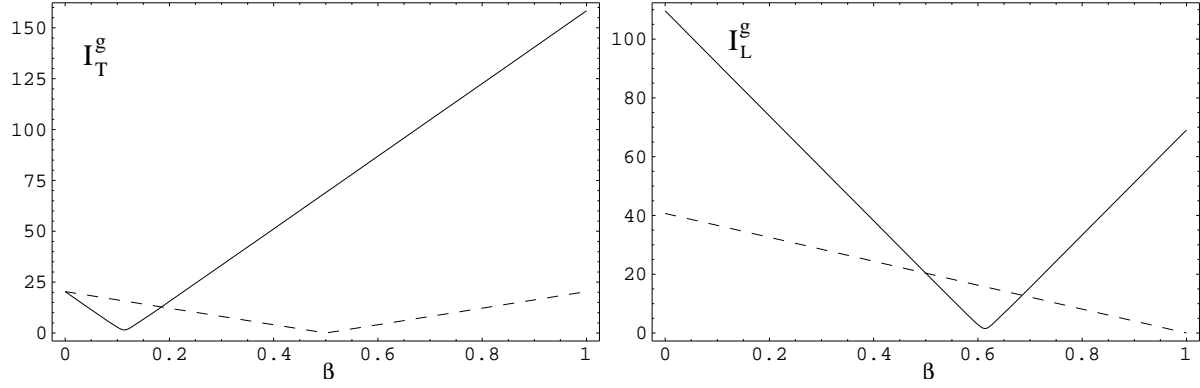


FIG. 13: The absolute values of I_T^g (left panel) and I_L^g (right panel) calculated for $\xi = 0.001$ and using the CTEQ6L parametrization for the gluon GPD for different values of β (16). The dashed curves represent the contributions of the double pole terms, see text.

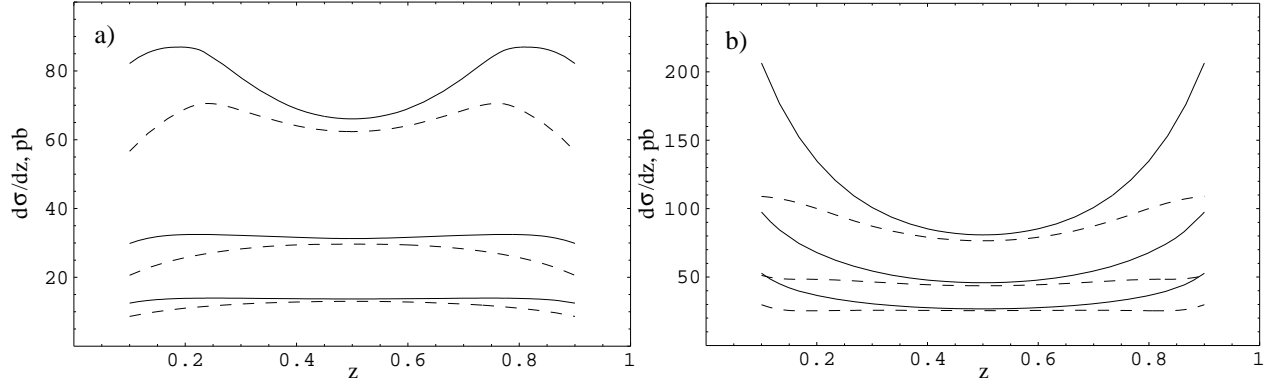


FIG. 14: Longitudinal momentum fraction distribution of the dijets, summed over the light quark flavors $q = u, d, s$. The three pair of curves correspond to different minimum dijet transverse momenta, from above to below: $q_0 = 1.25, 1.5, 1.75$ GeV. The solid and the dashed curves correspond to calculations when both the imaginary and the real part of the amplitude and when only the imaginary part of the amplitude is taken into account, respectively. The results shown on panel a) correspond to the calculation with a cutoff $\beta^{\text{DDIS}} > 0.5$, whereas the ones shown on panel b) are calculated without such a cutoff. In the latter case we take $Q^2 > 10 \text{ GeV}^2$.

- Rev. Lett. **86**, 4768 (2001).
- [13] D. Ashery [E791 Collaboration], arXiv:hep-ex/0205011.
- [14] L. Frankfurt, G. A. Miller and M. Strikman, Phys. Lett. B **304** (1993) 1.
- [15] V. M. Braun, S. Gottwald, D. Yu. Ivanov, A. Schafer and L. Szymanowski, Phys. Rev. Lett. **89**, 172001 (2002).
- [16] V. A. Khoze, A. D. Martin and M. G. Ryskin, Eur. Phys. J. C **23**, 311 (2002) [arXiv:hep-ph/0111078].
- [17] S. V. Goloskokov, Phys. Rev. D **70**, 034011 (2004).
- [18] M. Diehl, Z. Phys. C **76**, 499 (1997).
- [19] E. M. Levin, A. D. Martin, M. G. Ryskin and T. Teubner, Z. Phys. C **74**, 671 (1997).
- [20] J. Pumplin, D. R. Stump, J. Huston, H. L. Lai, P. Nadolsky and W. K. Tung, JHEP **0207**, 012 (2002)
- [21] A. D. Martin, R. G. Roberts, W. J. Stirling and R. S. Thorne, Phys. Lett. B **531**, 216 (2002).
- [22] A. V. Radyushkin, Phys. Rev. D **59**, 014030 (1999).
- [23] In the case $q_0 = 1.25$ and in the region $z \sim 1/2$ the cutoff $\beta^{\text{DDIS}} > 0.5$ is not effective since we assume, in any case, that $Q^2 \geq 10 \text{ GeV}^2$. For this reason the corresponding cross sections shown on both panels have similar magnitude and shape in the central region.
- [24] D. Yu. Ivanov, L. Szymanowski and G. Krasnikov, JETP Lett. **80**, 226 (2004) [Pisma Zh. Eksp. Teor. Fiz. **80**, 255 (2004)]; D. Yu. Ivanov, A. Schafer, L. Szymanowski and G. Krasnikov, Eur. Phys. J. C **34**, 297 (2004).